

## A Type of Finite Element Gradient Recovery Method based on Vertex-Edge-Face Interpolation: The Recovery Technique and Superconvergence Property

Qun Lin\* and Hehu Xie

*LSEC, ICMSEC, Academy of Mathematics and Systems Science, Chinese Academy of Sciences, Beijing 100190, China.*

*Received 25 December 2010; Accepted (in revised version) 25 April 2011*

*Available online 27 July 2011*

---

**Abstract.** In this paper, a new type of gradient recovery method based on vertex-edge-face interpolation is introduced and analyzed. This method gives a new way to recover gradient approximations and has the same simplicity, efficiency, and superconvergence properties as those of superconvergence patch recovery method and polynomial preserving recovery method. Here, we introduce the recovery technique and analyze its superconvergence properties. We also show a simple application in the a posteriori error estimates. Some numerical examples illustrate the effectiveness of this recovery method.

**AMS subject classifications:** 65N30, 65N12, 65N15, 65D10, 74S05

**Key words:** Finite element method, least-squares fitting, vertex-edge-face interpolation, superconvergence, a posteriori error estimate.

---

### 1. Introduction

Recently, a posteriori error estimates based on gradient recovery methods are active and attract more and more attention ([1–4, 8, 10, 12, 14–16, 20, 21, 23–25, 27]). One of the most widely used in practice is Zienkiewicz-Zhu's Superconvergence Patch Recovery (SPR) method ([27]) based on a local discrete least squares fitting. The popularity of this method relies on various factors: the method is rather independent of the problem, it is cheap to compute and easy to implement and the method works very well in practice. The robustness of the SPR method is dependent on its superconvergence property under structured meshes ([22]). However, [25] shows that the SPR is not superconvergence for linear element under the uniform triangulation of the Chevron pattern. The Polynomial Preserving Recovery (PPR) which overcomes this restriction is one of the most recent least-squares-based procedures ([16, 21, 24, 25]). This method is based on computing a local second order polynomial on a suitable patch associated with each mesh vertex via

---

\*Corresponding author. *Email addresses:* linq@lsec.cc.ac.cn (Q. Lin), hhxie@lsec.cc.ac.cn (H. Xie)

a discrete least-squares procedure. Then, the nodal gradient can be computed, which are family linearly interpolated. The PPR-recovered gradient has superconvergence properties in mildly structured meshes, and, in such cases, it was shown to be asymptotic exact ([21]). Both SPR and PPR select the node values as samples. The effectiveness of the gradient recovery method is rooted in the superconvergence theory. However, from the superconvergence theory ([12, 14, 15]), we know that the vertex-edge-face interpolations have better superconvergent properties than the common Lagrange interpolations. In this paper, a new type of gradient recovery method based on the vertex-edge-face interpolation is proposed and analyzed. The new gradient recovery method, given a finite element space of degree  $k$ , instead of gradient values at some sampling points on element patches (as in the SPR method and PPR method), selects gradient integration at the sampling edges and faces to obtain recovered gradient at each assembly vertex, edge and face. We shall prove that the new method has superconvergence for the superconvergent mesh (such as uniform triangular mesh of the Regular pattern and Chevron pattern, mildly meshes and so on) ([3, 6, 12, 14, 15, 21, 26]). In computer implementation, there is no significant difference between the new method with SPR or PPR compared with the overall cost in finite element solution.

The simple application of this recovery method to a posteriori error estimate is also discussed. The reader is referred to [1, 2] for analysis of recovery type a posteriori error estimators.

The paper is organized as follows. We give the recovery technique in Section 2 and Section 3 is devoted to the superconvergence analysis. Section 4 shows the application of the recovery method to a posteriori error estimate. Numerical results are presented in Section 5. Finally, Section 6 contains some concluding remarks.

## 2. The Finite Element Method and Recovery Technique

This section is devoted to the introduction of the recovery technique. For simplicity, we consider the second order elliptic problem: Find a scalar function  $u$  such that

$$-\nabla \cdot (\mathcal{A} \nabla u) + bu = f, \quad \text{in } \Omega, \quad (2.1)$$

$$u = u_D, \quad \text{on } \partial\Omega, \quad (2.2)$$

where  $\mathcal{A} \in \mathcal{R}^{2 \times 2}$  is a positive definite matrix in  $\Omega$ ,  $b \geq 0$  and  $\Omega \subset \mathcal{R}^2$  is a bounded domain with Lipschitz boundary  $\partial\Omega$ .

In order to use the finite element method to compute the problem (2.1)-(2.2), we need to introduce a triangulation  $\mathcal{T}_h$  on the domain  $\Omega$  and then define the finite element space  $S_h \subset H^1(\Omega)$  as

$$S_h = \{v \in H^1(\Omega) : v|_e \in \mathcal{P}_k(e), \quad \forall e \in \mathcal{T}_h\},$$

where  $\mathcal{P}_k(e)$  is the space of polynomials of degree not greater than a positive integer  $k$ . The finite element method is to find  $u_h \in S_h^D$  such that

$$a(u_h, v) = (f, v), \quad \forall v \in S_h, \quad (2.3)$$

where

$$a(u, v) = \int_{\Omega} (\nabla u \cdot \mathcal{A} \nabla v + buv) dx dy,$$

$$(f, v) = \int_{\Omega} f v dx dy,$$

and  $S_h^D$  denote the set of the functions in  $S_h$  satisfying the boundary condition (2.2).

We will introduce a new gradient recovery operator  $G_h : S_h \rightarrow S_h \times S_h$ . First, let us introduce the vertex-edge-face interpolation of degree  $k$  for  $u \in H^{1+\epsilon}(e)$  as follows

$$u_I(Z_i) = u(Z_i), i = 1, 2, 3, \quad (2.4a)$$

$$\int_{l_i} u_I v ds = \int_{l_i} u v ds, \forall v \in \mathcal{P}_{k-2}(l_i), i = 1, 2, 3, \quad (2.4b)$$

$$\int_e u_I v dx dy = \int_e u v dx dy, \quad \forall v \in \mathcal{P}_{k-3}(e), \quad (2.4c)$$

where  $Z_i$  and  $l_i$  are the three vertices and three edges of element  $e$  and  $\epsilon$  is an arbitrary small positive number. From the interpolation definition, the number of equations is  $3 + 3(k-1) + (k-1)(k-2)/2 = (k+1)(k+2)/2$  which equals the dimension of  $\mathcal{P}_k(e)$ .

In the superconvergence theory, it has been proved that this type of interpolation has better superconvergent property than the common Lagrange interpolation especially for high order finite element method. For example, this type of interpolation has very beautiful interpolation expansions by the integral identity or integral expansion ([11, 12, 14, 15]). From the definition, we can know there are three kinds of degree of freedom: vertex value, edge integration and face integration. The gradient recovery procedure aims to obtain these three kinds of degree of freedom.

Now, let's introduce the gradient recovery procedure. Given a finite element solution  $u_h$ , we need to define  $G_h u_h$  at the following three types of degree of freedom: vertex value, edge integration, and face integration. For the linear element all degrees of freedom are vertex values, for the quadratic element they are vertex values and edge integrations, and for the cubic element all three types of degrees of freedom are presented. After determining values of  $G_h u_h$  at all degrees of freedom, we obtain  $G_h u_h \in S_h \times S_h$  on the whole domain by interpolation with the original shape functions of  $S_h$ .

## 2.1. Step 1

We start from vertices. For a vertex  $Z_i$ , let  $h_i$  be the length of the longest edge attached to  $Z_i$ . Elements which include  $Z_i$  are selected to form the patch  $\omega_i$

$$\omega_i = \bigcup_{Z_i \in e \in \mathcal{T}_h} e.$$

Let  $\mathcal{E}_{Z_i}$  denote the element edges set on the patch  $\omega_i$ . We fit a two dimensional polynomial vector of degree  $k$ , in the least-squares sense, to the gradient of the finite element solution  $u_h$  at the degrees of freedom: edge and face integrations.

First, we define the affine transformation  $F : (x, y) \mapsto (\xi, \eta)$ :

$$\xi = \frac{x - x_i}{h}, \quad \eta = \frac{y - y_i}{h}, \quad (2.5)$$

where  $(x_i, y_i)$  is the coordination of  $Z_i$  and  $h = h_i$ . In order to eliminate unstability, we implement the recovery process in the reference patch

$$\widehat{\omega}_i = F\omega_i = \bigcup_{Z_i \in e \in \mathcal{T}_h} Fe.$$

Then, we set  $\widehat{\nabla}u_h(\xi, \eta) = \nabla u_h(x, y)$ ,  $\widehat{\mathbf{v}}(\xi, \eta) = \mathbf{v}(x, y)$ . Now, let's define a functional for any polynomial vector  $\widehat{\mathbf{v}} \in (\mathcal{P}_k(\widehat{\omega}_i))^2$  by

$$\begin{aligned} \mathcal{F}(\widehat{\mathbf{v}}) = & \sum_{\widehat{e} \in \widehat{\omega}_i} \sum_{0 \leq m+j \leq k-2} \left( \left[ \int_{\widehat{e}} \widehat{\mathbf{v}} \cdot (\xi^m \eta^j, 0)^T d\xi d\eta \right]^2 + \left[ \int_{\widehat{e}} \widehat{\mathbf{v}} \cdot (0, \xi^m \eta^j)^T d\xi d\eta \right]^2 \right) \\ & + \sum_{\widehat{l} \in \widehat{\mathcal{E}}_{Z_i}} \sum_{j=0}^{k-1} \left[ \int_{\widehat{l}} \widehat{\mathbf{v}} \cdot \widehat{\mathbf{t}}_l \widehat{s}^j d\widehat{s} \right]^2, \end{aligned} \quad (2.6)$$

where  $\widehat{\mathbf{t}}_l$  denotes the reference unity tangent vector of the corresponding edge and  $\widehat{\mathcal{E}}_{Z_i}$  denotes the element edges set on the reference patch  $\widehat{\omega}_i$ , and  $\widehat{e}$  the element in  $\widehat{\omega}_i$ .

In order to implement the recovery procedure, we introduce the following notations

$$\widehat{\mathbf{P}}_k = \begin{pmatrix} \widehat{\mathbf{P}}_k^T & \mathbf{0}_n^T \\ \mathbf{0}_n^T & \widehat{\mathbf{P}}_k^T \end{pmatrix},$$

where

$$\widehat{\mathbf{P}}_k^T = (1, \xi, \eta, \xi^2, \dots, \xi^k, \xi^{k-1}\eta, \dots, \eta^k)$$

and  $\mathbf{0}_n$  denote the vector whose elements are all 0 with  $n = (k+1)(k+2)/2$ . The fitting polynomial vector is denoted by

$$\widehat{\boldsymbol{\sigma}}_k(\xi, \eta; Z_i) = \widehat{\mathbf{P}}_k \widehat{\mathbf{a}}$$

with

$$\widehat{\mathbf{a}}^T = (\widehat{a}_1, \widehat{a}_2, \dots, \widehat{a}_{2n}).$$

Then, the fitting polynomial vector  $\widehat{\boldsymbol{\sigma}}_k$  can be determined by minimizing the following functional problem

$$\mathcal{F}(\widehat{\boldsymbol{\sigma}}_k - \widehat{\nabla}u_h) = \min_{\widehat{\mathbf{v}} \in (\mathcal{P}_k(\widehat{\omega}_i))^2} \mathcal{F}(\widehat{\mathbf{v}} - \widehat{\nabla}u_h). \quad (2.7)$$

**Remark 2.1.** Of course, in order to reduce the dimensions of the minimization problem (2.7), we can also modify this functional problem into the following similar version

$$\mathcal{F}(\nabla \widehat{\sigma}_{k+1} - \nabla u_h) = \min_{v \in \mathcal{P}_{k+1}(\widehat{\omega}_i)} \mathcal{F}(\nabla \widehat{v} - \nabla u_h),$$

where  $\widehat{\sigma}_{k+1} \in \mathcal{P}_{k+1}(\widehat{\omega}_i)$ .

The minimization problem (2.7) yields the following linear system

$$A^T A \widehat{\mathbf{a}} = A^T \widehat{\mathbf{b}}_h. \quad (2.8)$$

After solving the linear system, we obtain the coefficient vector  $\widehat{\mathbf{a}}$  and then the polynomial vector  $\widehat{\sigma}_k(\xi, \eta; Z_i)$ . The final fitted polynomial can be obtained by

$$\sigma_k(x, y; Z_i) = \widehat{\sigma}_k \left( \frac{x - x_i}{h}, \frac{y - y_i}{h}; Z_i \right).$$

The condition for (2.8) to have a unique solution is

$$\text{Rank}A = 2n, \quad (2.9)$$

which is always satisfied in practical situation when grid points are reasonably distributed. Then, we define

$$G_h u_h(Z_i) = \sigma_k(x, y; Z_i)(Z_i). \quad (2.10)$$

## 2.2. Step 2

For the degree of freedom on the edge  $l$  between two vertices  $Z_{i_1}$  and  $Z_{i_2}$ , we define

$$\int_l G_h u_h \mathbf{v} ds = \frac{1}{2} \left( \int_l \sigma_k(x_1, y_1; Z_{i_1}) \mathbf{v} ds + \int_l \sigma_k(x_2, y_2; Z_{i_2}) \mathbf{v} ds \right), \forall \mathbf{v} \in (\mathcal{P}_{k-2}(l))^2, \quad (2.11)$$

where  $(x_1, y_1)$  (or  $(x_2, y_2)$ ) is the local coordinate on the edge with origin at  $Z_{i_1}$  (or  $Z_{i_2}$ ).

## 2.3. Step 3

For the degree of freedom on the face  $e$  which formed by three vertices  $Z_{i_1}, Z_{i_2}$  and  $Z_{i_3}$ , we define

$$\int_e G_h u_h \mathbf{v} dx dy = \frac{1}{3} \sum_{j=1}^3 \int_e \sigma_k(x_j, y_j; Z_{i_j}) \mathbf{v} dx dy, \quad \forall \mathbf{v} \in (\mathcal{P}_{k-3}(e))^2, \quad (2.12)$$

where  $(x_j, y_j)$  are the local coordinates on the face  $e$  with origin at  $Z_{i_j}$ , respectively.

**Remark 2.2.** We use criteria (2.11) and (2.12) to make the recovery process be consistent with the vertex-edge-face interpolation definition and its shape functions. Of course, the direct average of the corresponding vector polynomials  $\sigma_k$  can also be used.

After determining values of  $G_h u_h$  at all the degrees of freedom,  $G_h u_h$  can be constructed by interpolation with the original shape functions of  $S_h$ . In order to demonstrate the method more clearly, here we discuss two examples in detail. For the sake of simplicity, both examples are under uniform meshes. Nevertheless, we can find the method can be applied to arbitrary meshes even with curved boundaries.

**Example 2.1.** Linear element on the uniform triangulation of the Regular pattern. Let the length of the horizontal and vertical edge of the element patch (see Fig. 1) be  $h$  and we scale the patch by the factor  $h$  with  $x = h\xi, y = h\eta$ . Equivalently, we fit a linear polynomial vector

$$\boldsymbol{\sigma}_1(x, y; Z_i) = \mathbf{P}_1 \mathbf{a}$$

minimizing the following functional

$$\sum_{l \in \mathcal{E}_{Z_i}} \left[ \int_l \left( \frac{\partial u_h}{\partial \mathbf{t}_l} - \boldsymbol{\sigma}_1 \cdot \mathbf{t}_l \right) ds \right]^2 = \min_{\mathbf{v} \in (\mathcal{P}_1(\omega_i))^2} \left\{ \sum_{l \in \mathcal{E}_{Z_i}} \left[ \int_l \left( \frac{\partial u_h}{\partial \mathbf{t}_l} - \mathbf{v} \cdot \mathbf{t}_l \right) ds \right]^2 \right\}, \quad (2.13)$$

where

$$\mathbf{P}_1 = \begin{pmatrix} 1 & x & y & 0 & 0 & 0 \\ 0 & 0 & 0 & 1 & x & y \end{pmatrix},$$

The fitting procedure results in  $A^T \mathbf{A} \mathbf{a} = A^T \mathbf{b}$ . It is straightforward to calculate

$$(A^T A)^{-1} A^T = \frac{1}{12} \begin{pmatrix} 2 & 2 & 2 & 2 & 1 & 1 & 1 & 1 & 1 & 1 & 1 & 1 \\ 0 & -6 & 6 & 0 & -3 & 3 & -3 & 3 & -3 & 3 & -3 & 3 \\ 5 & -3 & 3 & -5 & -1 & 3 & -3 & 1 & -2 & 2 & 0 & 0 \\ 1 & 1 & 1 & 1 & 2 & 2 & 2 & 2 & -1 & -1 & -1 & -1 \\ 1 & -3 & 3 & -1 & -5 & 3 & -3 & 5 & 2 & -2 & 0 & 0 \\ 3 & -3 & 3 & -3 & 0 & 6 & -6 & 0 & 3 & -3 & -3 & 3 \end{pmatrix}.$$

After obtaining the vector  $\mathbf{b}$ , the fitted linear polynomial vector at  $(0, 0)$  (it means the vertex  $Z_i$ ) is

$$\frac{1}{6h} \begin{pmatrix} 2(u_3 - u_6) + u_4 - u_5 + u_2 - u_1 \\ 2(u_4 - u_1) + u_5 - u_6 + u_3 - u_2 \end{pmatrix}. \quad (2.14)$$

By the Taylor expansion, it can be verified directly that (2.14) provide the second order approximation to  $\nabla u$  at the original vertex  $Z_i$  which is displayed in Fig. 1. With  $G_h u$  given at each vertex by (2.14), we can construct a recovered gradient field by linear interpolation using linear finite element basis functions. This result is the same as SPR and PPR.

**Example 2.2.** Linear element on the uniform triangulation of the Chevron pattern. Following the same procedure as Example 2.1, we can obtain the recovered gradient at the vertex  $Z_i$  (see Fig. 2)

$$\frac{1}{22h} \begin{pmatrix} u_4 - u_6 \\ -4u_0 - 2u_1 - 7u_2 - 2u_3 + 2u_4 + 11u_5 + 2u_6 \end{pmatrix}. \tag{2.15}$$

We also know this gives a second order approximation to the gradient and is different with SPR and PPR. SPR can not give a second order approximation to the gradient and the scheme determined by PPR is different with (2.15) ([25]) on the uniform triangulation of the Chevron pattern.

As same as SPR and PPR, recovering the gradient on the boundary is more complicated,

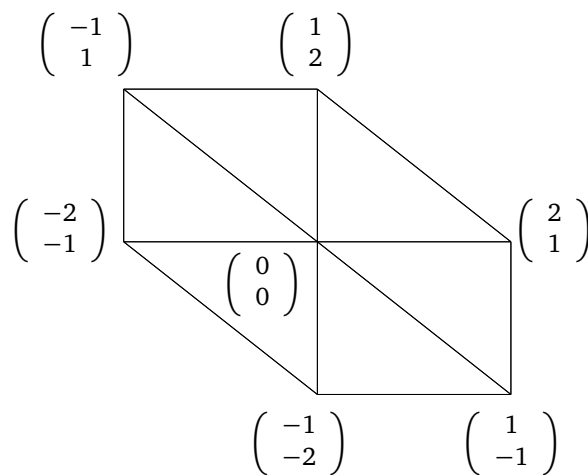


Figure 1: The patch for the uniform mesh of Regular pattern.

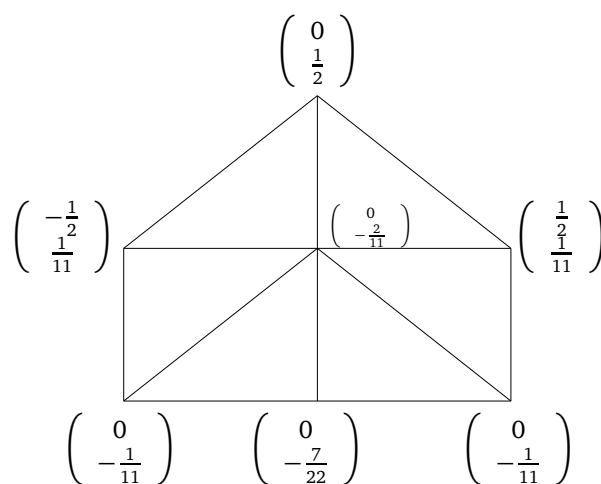


Figure 2: The patch for the uniform mesh of Chevron pattern.

although there are many ways to deal with that. The obvious way is to use the strategy adopt for internal vertices. However, as in [25], our computational experiments indicated that this strategy is not efficient. To overcome this shortcoming, we look for the nearest layer of vertices around  $Z$  that contains at least one internal vertex to recover the gradient at a vertex  $Z \in \partial\Omega$ . Let this layer be the  $r$ -th one, and denote the internal vertices in this layer by  $Z_1, Z_2, \dots, Z_m$  where  $m > 1$ . The union of the patches used in recovering the gradient at  $Z_1, Z_2, \dots, Z_m$ , and the elements in the first  $r$  layers around  $Z$  constitute the patch for recovering the gradient at  $Z$ .

If the unique solution condition (2.9) violates, we need to extend the patch to include more elements until the rank condition (2.9) is satisfied.

### 3. Superconvergence Analysis

In this section, we give the superconvergence analysis of our recovery operator with the tools in [12, 14, 15]. We refer readers to [5, 7] for general theory of the finite element method and to [6, 12, 14, 15, 18, 26] for the superconvergence theory. Since there are many papers concerning the superconvergence analysis of our recovery methods, we only give the outline for the superconvergence of the new recovery method. Readers who are interested in the details are referred to the related references.

First, we find the recovery operator has the following properties.

**Theorem 3.1.** *The recovery operator  $G_h$  defined in this paper satisfies*

$$\|G_h u_h\|_0 \leq C \|u_h\|_1, \quad \forall u_h \in S_h, \quad (3.1)$$

$$G_h v = \nabla v, \quad \forall v \in \mathcal{P}_{k+1}(\omega_i), \quad (3.2)$$

$$G_h v = G_h v_I. \quad (3.3)$$

*Proof.* Proofs for (3.1) and (3.2) are trivial ([12, 14, 15]). For convenient reading, we give their proofs.

First, we prove  $\mathcal{F}(\hat{\mathbf{v}})^{1/2}$  defines a norm for  $\hat{\mathbf{v}} \in (\mathcal{P}_k(\hat{\omega}_i))^2$  on the reference patch  $\hat{\omega}_i$ . When the rank condition (2.9) is satisfied, we know  $\mathcal{F}(\hat{\mathbf{v}})^{1/2} = 0$  if and only if  $\hat{\mathbf{v}} = 0$ . And from the finity of the dimension of the polynomial vector space, norm equivalence theorem and the regularity of the triangulation  $\mathcal{T}_h$ , we can know there exist constants  $C_1$  and  $C_2$  which are independent of  $h$  such that

$$C_1 \|\hat{\mathbf{v}}\|_{0, \hat{\omega}_i} \leq \mathcal{F}(\hat{\mathbf{v}})^{1/2} \leq C_2 \|\hat{\mathbf{v}}\|_{0, \hat{\omega}_i}.$$

Based on this result and the minimization problem (2.7), we can know

$$\|\hat{\boldsymbol{\sigma}}_k\|_{0, \hat{\omega}_i} \leq 1/C_1 \mathcal{F}(\hat{\boldsymbol{\sigma}}_k)^{1/2} \leq 1/C_1 \mathcal{F}(\widehat{\nabla} u_h)^{1/2} \leq C_2/C_1 \|\widehat{\nabla} u_h\|_{0, \hat{\omega}_i}.$$

Combination with the definition of the transformation  $F$ , the following inequality can be obtained

$$\|\boldsymbol{\sigma}_k\|_{0, \omega_i} \leq C_2/C_1 \|\nabla u_h\|_{0, \omega_i}. \quad (3.4)$$

For any element  $e$ , let  $Z_1, Z_2$  and  $Z_3$  denote its three vertices. From the recovery process and (3.4), we can obtain the following inequality

$$\|G_h u_h\|_{0,e} \leq C \sum_{i=1}^3 \|\sigma_k(x, y; Z_i)\|_{0,\omega_i} \leq C \sum_{i=1}^3 \|\nabla u_h\|_{0,\omega_i}. \tag{3.5}$$

Then from (3.5) and summing over the mesh, we have

$$\|G_h u_h\|_0^2 = \sum_{e \in \mathcal{T}_h} \|G_h u_h\|_{0,e}^2 \leq C \sum_{e \in \mathcal{T}_h} \sum_{i=1}^3 \|\nabla u_h\|_{0,\omega_i}^2 \leq C \|\nabla u_h\|_0^2.$$

So (3.1) can be obtained.

For the property (3.2), we should notice that  $\nabla v \in (\mathcal{P}_k(\omega_i))^2$  when  $v \in \mathcal{P}_{k+1}(\omega_i)$  on a patch  $\omega_i$ . From the function definition (2.6) and the minimizing function problem (2.7), we can know the fitting polynomial  $\sigma_k(x, y; Z_i) = \nabla v$  on the patch  $\omega_i$ . Then, the property (3.2) can be obtained.

For (3.3), we need to prove  $G_h(v - v_I) = 0$ . This can be ensured by

$$\begin{aligned} \int_l \frac{\partial(v - v_I)}{\partial \mathbf{t}_l} \varphi ds &= (v - v_I) \varphi \Big|_{Z_{i_1}}^{Z_{i_2}} - \int_l (v - v_I) \frac{\partial \varphi}{\partial \mathbf{t}_l} ds = 0, \\ &\quad \forall \varphi \in \mathcal{P}_{k-1}(l), \\ \int_e \nabla(v - v_I) \cdot \mathbf{w} dx dy &= \int_{\partial e} (v - v_I) \mathbf{n} \cdot \mathbf{w} ds - \int_e (v - v_I) \nabla \cdot \mathbf{w} dx dy = 0, \\ &\quad \forall \mathbf{w} \in (\mathcal{P}_{k-2}(e))^2, \end{aligned}$$

for each edge  $l$  between  $Z_{i_1}$  and  $Z_{i_2}$  and each face  $e$ . This is a smart representation for the definition of the vertex-edge-face interpolation and shows that the recovery method has the property (3.3). □

Since there are many ways to analyze finite element superconvergence ([3,6,12,14,15,17–19,21,26]), here we just construct a framework for the superconvergence of the new recovery method. Based on Theorem 3.1, if the mesh has the superconvergence property ([3,14,17,21]), we can obtain the superconvergence result after recovering the gradient.

**Theorem 3.2.** *If the following superapproximation exists*

$$\|u_h - u_I\|_1 \leq Ch^{k+\delta}, \tag{3.6}$$

where  $\delta \in (0, +\infty)$ . Then, we have the superconvergence result

$$\|G_h u_h - \nabla u\|_0 \leq Ch^{k+\min\{1,\delta\}}. \tag{3.7}$$

*Proof.* Combining Theorem 3.1 and (3.6), we have

$$\begin{aligned} \|G_h u_h - \nabla u\|_0 &\leq \|G_h u_h - G_h u_I\|_0 + \|G_h u_I - G_h u\|_0 + \|G_h u - \nabla u\|_0 \\ &\leq C \|u_h - u_I\|_1 + Ch^{k+1} \\ &\leq Ch^{k+\min\{1,\delta\}}. \end{aligned}$$

This is the desired result and we complete the proof.  $\square$

In practical computation, the mesh always has superconvergence property more or less (means that on the mesh there exists the superconvergence (3.7) with  $\delta > 0$  ([13] and [3, 6, 10, 12, 14, 16, 21, 22])). This is the reason why the finite element postprocessing method can often improve the accuracy of the solution. This observation has been confirmed by large number of numerical tests.

#### 4. Application in the a Posteriori Error Estimate

With the recovery method proposed in this paper, we can construct an a posteriori error estimator. By the recovery gradient  $G_h u_h$ , a posteriori error estimator can then be defined as

$$\eta_e = \|G_h u_h - \nabla u_h\|_{0,e}, \quad \eta_\Omega = \left( \sum_{e \in \mathcal{T}_h} \eta_e^2 \right)^{1/2} = \|G_h u_h - \nabla u_h\|_0. \quad (4.1)$$

If the recovery gradient  $G_h u_h$  has superconvergence property

$$\|\nabla u - G_h u_h\|_0 \ll \|\nabla u - \nabla u_h\|_0, \quad (4.2)$$

the a posteriori error estimator  $\eta_\Omega$  is asymptotic exact. Indeed, by the triangular inequality

$$1 - \frac{\|\nabla u - G_h u_h\|_0}{\|\nabla u - \nabla u_h\|_0} \leq \frac{\|G_h u_h - \nabla u_h\|_0}{\|\nabla u - \nabla u_h\|_0} \leq 1 + \frac{\|\nabla u - G_h u_h\|_0}{\|\nabla u - \nabla u_h\|_0}.$$

By virtue of (4.2),  $\|\nabla u - G_h u_h\|_0 / \|\nabla u - \nabla u_h\|_0$  is much smaller comparing with 1. Therefore

$$\frac{\|G_h u_h - \nabla u_h\|_0}{\|\nabla u - \nabla u_h\|_0} \approx 1.$$

Based on the a posteriori error estimator (4.1), we can construct an adaptive finite element method to solve some singular problems ([24, 27]).

#### 5. Numerical Tests

In this section, three test problems are used to verify superconvergence of the new recovery method. Here, we first give the numerical results for the elliptic problem by the linear element on the uniform meshes of the four patterns: Regular, Chevron, Criss Cross, and Union Jack. The aim of this example is to investigate the superconvergence of the new recovery method under the uniform meshes. Then, we give the numerical results by the linear element on the general mesh which generated by Delaunay triangulation. In this example, we want to investigate the effectiveness of the new recovery method on the general unstructured meshes. In the third example, recovery method is applied to adaptive finite element method by constructing a posteriori error estimates.

Table 1: The uniform triangular mesh of Regular pattern.

| Mesh                          | 10 × 10 | 20 × 20  | 40 × 40   | 60 × 60   |
|-------------------------------|---------|----------|-----------|-----------|
| $\ \nabla u - \nabla u_h\ _0$ | 0.34408 | 0.17401  | 0.087189  | 0.058144  |
| Rate                          | /       | /        | /         | 0.99325   |
| $\ G_h u_h - \nabla u\ _0$    | 0.13579 | 0.034876 | 0.0087986 | 0.0039197 |
| Rate                          | /       | /        | /         | 1.9906    |

Table 2: The uniform triangular mesh of Chevron pattern.

| Mesh                          | 10 × 10 | 20 × 20  | 40 × 40   | 60 × 60   |
|-------------------------------|---------|----------|-----------|-----------|
| $\ \nabla u - \nabla u_h\ _0$ | 0.34356 | 0.17392  | 0.087176  | 0.058141  |
| Rate                          | /       | /        | /         | 0.99253   |
| $\ G_h u_h - \nabla u\ _0$    | 0.13311 | 0.030463 | 0.0071234 | 0.0030861 |
| Rate                          | /       | /        | /         | 2.0956    |

Table 3: The uniform triangular mesh of Criss Cross pattern.

| Mesh                          | 10 × 10  | 20 × 20  | 40 × 40   | 60 × 60   |
|-------------------------------|----------|----------|-----------|-----------|
| $\ \nabla u - \nabla u_h\ _0$ | 0.18329  | 0.091908 | 0.045974  | 0.030651  |
| Rate                          | /        | /        | /         | 0.99837   |
| $\ G_h u_h - \nabla u\ _0$    | 0.076907 | 0.019296 | 0.0048235 | 0.0021432 |
| Rate                          | /        | /        | /         | 1.9986    |

Table 4: The uniform triangular mesh of Union Jack pattern.

| Mesh                          | 10 × 10 | 20 × 20  | 40 × 40  | 60 × 60   |
|-------------------------------|---------|----------|----------|-----------|
| $\ \nabla u - \nabla u_h\ _0$ | 0.32627 | 0.1642   | 0.082215 | 0.054822  |
| Rate                          | /       | /        | /        | 0.99601   |
| $\ G_h u_h - \nabla u\ _0$    | 0.22002 | 0.057093 | 0.014401 | 0.0064115 |
| Rate                          | /       | /        | /        | 1.9764    |

**Example 5.1.** The first example is to solve

$$\begin{aligned}
 -\Delta u &= 2\pi^2 \sin \pi x \sin \pi y, & \text{in } \Omega &= [0, 1] \times [0, 1], \\
 u &= 0, & \text{on } \partial\Omega.
 \end{aligned}$$

The exact solution is  $u(x, y) = \sin \pi x \sin \pi y$ . Here, we consider the linear element on the four patterns of uniform triangular meshes.

As mentioned earlier, for the linear element, the new recovery method has the same superconvergence as the SPR and PPR under the uniform triangular mesh of the Regular pattern. From Table 2, we can find that the new method provides superconvergence on the uniform triangulation of Chevron pattern as same as PPR. For structured meshes, the new recovery method has very good superconvergence properties (see Tables 1, 2, 3 and 4).

Table 5: Numerical results for the mesh produced by regular refinement.

| Mesh                          | $\mathcal{T}_{0.1}$ | $\mathcal{T}_{0.1/2}$ | $\mathcal{T}_{0.1/4}$ | $\mathcal{T}_{0.1/8}$ |
|-------------------------------|---------------------|-----------------------|-----------------------|-----------------------|
| $\ \nabla u - \nabla u_h\ _0$ | 0.43421             | 0.21891               | 0.10968               | 0.054853              |
| Rate                          | /                   | /                     | /                     | 0.99491               |
| $\ G_h u_h - \nabla u\ _0$    | 0.12401             | 0.036524              | 0.010463              | 0.0030253             |
| Rate                          | /                   | /                     | /                     | 1.7857                |

Table 6: The general mesh produced by Delauny triangulation.

| Mesh                          | $\mathcal{T}_{0.1}$ | $\mathcal{T}_{0.05}$ | $\mathcal{T}_{0.025}$ | $\mathcal{T}_{0.0125}$ |
|-------------------------------|---------------------|----------------------|-----------------------|------------------------|
| $\ \nabla u - \nabla u_h\ _0$ | 0.43421             | 0.21474              | 0.10728               | 0.053554               |
| $\ G_h u_h - \nabla u\ _0$    | 0.12401             | 0.097541             | 0.023299              | 0.0041281              |

**Example 5.2.** The second example is to solve

$$\begin{aligned} -\nabla \cdot (\mathcal{A} \nabla u) &= f, & \text{in } \Omega, \\ u &= 0, & \text{on } \partial\Omega, \end{aligned}$$

where

$$\mathcal{A} = \begin{pmatrix} e^{x^2+1} & e^{xy} \\ e^{xy} & e^{y^2} \end{pmatrix}.$$

The exact solution is also  $u(x, y) = \sin \pi x \sin \pi y$ . For this example, the initial mesh is unstructured which is produced by Delauny triangulation (see Fig. 3). Table 5 is the numerical results on the successive meshes produced by regular refinement (by linking edge midpoints) of initial mesh. Table 6 lists the numerical results for each level mesh produced by Delauny triangulation directly and without regular refinement.

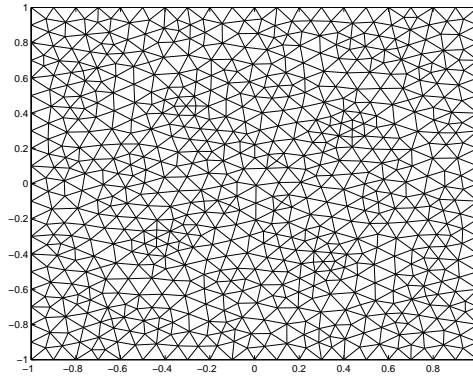


Figure 3: The initial mesh produced by Delauny triangulation.

Tables 5 and 6 show that the new recovery method can improve the accuracy of the finite element solution obviously on unstructured meshes. In the numerical tests, we also find that the effectiveness for the interior domain is better than the boundary layer.

**Example 5.3.** The third example is to solve the following Poisson equation

$$\begin{aligned} -\Delta u &= 0, & \text{in } \Omega, \\ u &= u_D, & \text{on } \partial\Omega, \end{aligned}$$

where  $\Omega = (-1, 1) \times (-1, 1) \setminus (0, 1) \times (-1, 0)$ ,  $u = r^{\frac{2}{3}} \sin(\frac{2}{3}\theta)$  and  $u_D$  denotes the Dirichlet boundary condition.

In order to deal with the reentrant corner singularity of this problem, we need to use adaptive finite element method. Here, the recovery method proposed in this paper is applied to construct the a posteriori error estimator ([24, 27]). In this example, we give two cases: regular initial mesh (Fig. 4) and irregular initial mesh (Fig. 6). The corresponding numerical results are shown in Fig. 5 and Fig. 7.

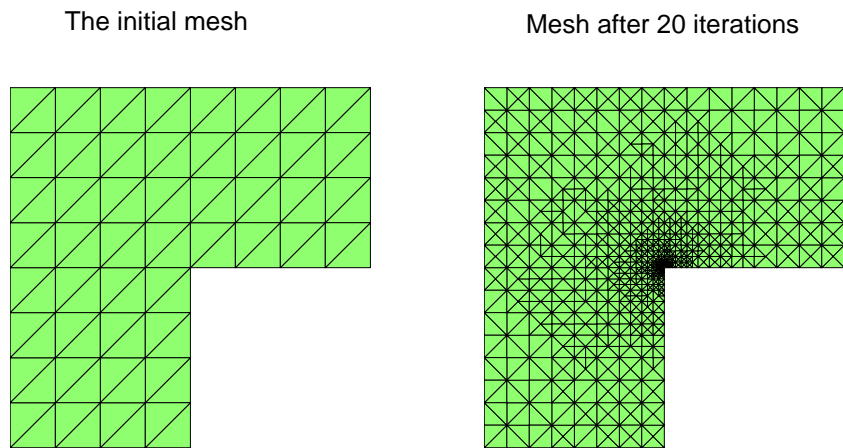


Figure 4: The regular initial mesh and the mesh after 20 adaptive iterations.

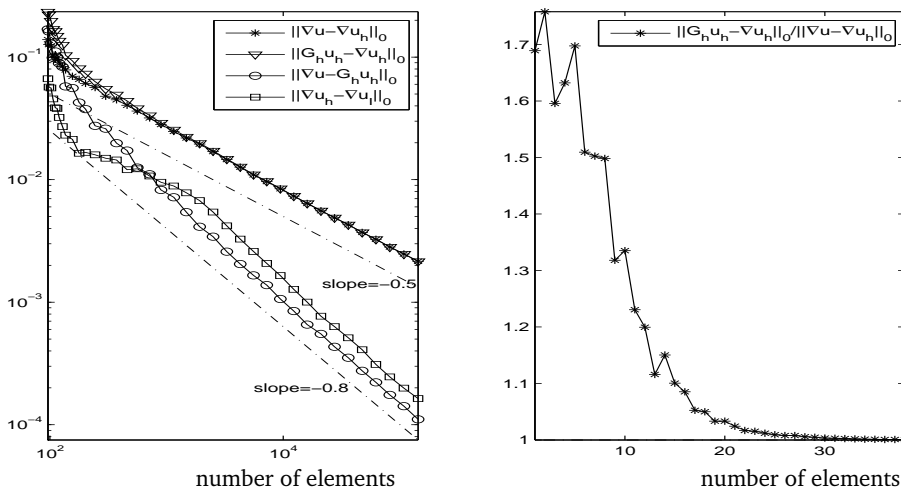


Figure 5: The convergence result for the regular initial mesh.

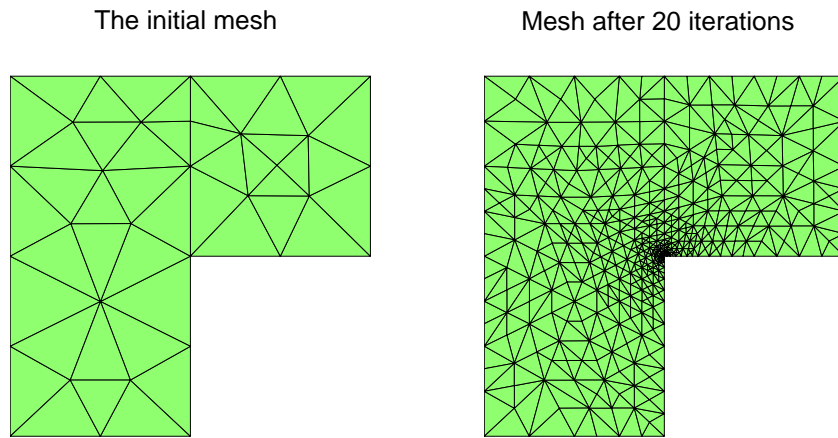


Figure 6: The irregular initial mesh and the mesh after 20 adaptive iterations.

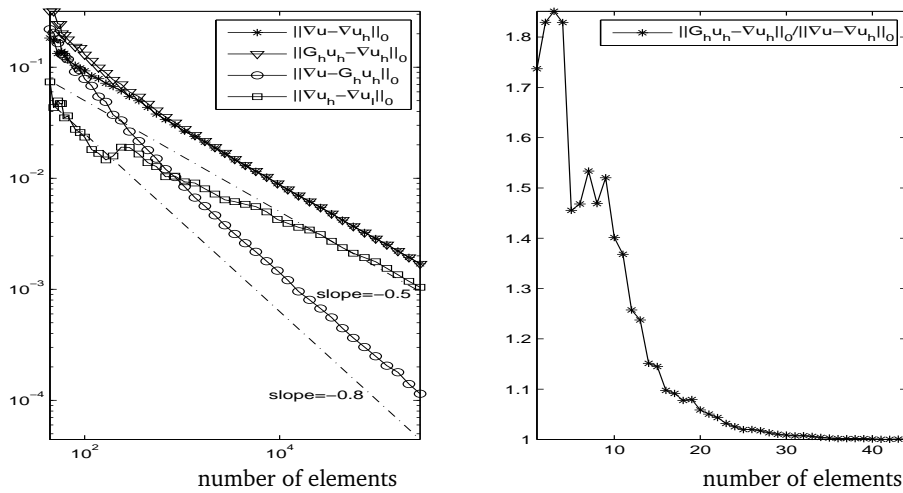


Figure 7: The convergence result for the irregular initial mesh.

From Figs. 4 and 5, we can find there exists superapproximation and superconvergence in the regular initial mesh case simultaneously. But from Figs. 6 and 7, there exists superconvergence even though there is no obvious superapproximation in the irregular mesh case. In both cases, the recovery method can give very efficient a posteriori error estimates.

### 6. Concluding Remarks

In summary, the new recovery method here keeps all known superconvergence properties of SPR and PPR. From the definition of the new recovery, we know that it has the same superconvergence property as PPR for linear element and our forthcoming consideration will be devoted to testing this method for high order finite elements. The idea of this type

of postprocessing technique can also be applied to that kind of interpolation which is based on the edge integration and (or) face integration such as the interpolations of mixed finite elements and Nédélec element. Of course, our further investigation will be devoted to the analysis of the application of the new recovery method to a posteriori error estimates and adaptive finite element methods under unstructured meshes, especially anisotropic meshes.

### Acknowledgments

This work is supported in part by the National Science Foundation of China (NSFC 11001259).

### References

- [1] M. Ainsworth and J. T. Oden, *A Posteriori Error Estimation in Finite Element Analysis*, Wiley Interscience, New York, 2000.
- [2] I. Babuška and T. Strouboulis, *The Finite Element Method and Its Reliability*, Oxford University Press, London, 2001.
- [3] R. E. Bank and J. Xu, Asymptotic exact a posteriori error estimators, Part I: Grids with superconvergence, *SIAM. J. Numer. Anal.*, 41(6) (2003), 2294-2312.
- [4] J. H. Bramble and A. H. Schatz, Higher order local accuracy by averaging in the finite element method, *Math. Comp.*, 31 (1977), 94-111.
- [5] S. C. Brenner and L. R. Scott, *The Mathematical Theory of Finite Element Methods*, Springer-Verlag, New York, 1994.
- [6] C. Chen and Y. Huang, *High Accuracy Theory for Finite Element Methods*, Hunan Sci. Tech. Press, China, 1995.
- [7] P. G. Ciarlet, *The finite Element Method for Elliptic Problem*, North-holland Amsterdam, 1978.
- [8] M. Křížek, P. Neittaanmäki and R. Stenberg (EDs.), *Finite Element Methods: Superconvergence, Post-processing, and A Posteriori Estimates*, Lecture Notes in Pure and Applied Mathematics Series, Vol. 196, Marcel Dekker, New York, 1997.
- [9] B. Li, superconvergence for higher-order triangular finite elements, *Chinese J. Numer. Math. Appl. (English)*, 12(1) (1990), 75-79.
- [10] B. Li and Z. Zhang, Analysis of a class of superconvergence patch recovery techniques for linear and bilinear finite elements, *Numer. Methods PDEs*, 15 (1999), 151-167.
- [11] J. Li, Convergence and superconvergence analysis of finite element methods on highly nonuniform anisotropic meshes for singularly perturbed reaction-diffusion problems, *Appl. Numer. Math.*, 36(2-3) (2001), 129-154.
- [12] Q. Lin and J. Lin, *Finite Element Methods: Accuracy and Improvement*, China Sci. Tech. Press, 2005.
- [13] Q. Lin and H. Xie, Superconvergence measurement for general meshes by linear finite element method, *Math. Pract. Theory*, 41(1) (2011), 138-152 (In Chinese).
- [14] Q. Lin and N. Yan, *The Construction and Analysis of High Efficiency Finite Element Methods*, HeBei University Publishers, P.R. China, 1995.
- [15] Q. Lin and Q. Zhu, *Preprocessing and Postprocessing for the Finite Element Method* (in Chinese), Shanghai Scientific & Technical Press, 1994.

- [16] A. Naga and Z. Zhang, A Posteriori error estimates based on the polynomial preserving recovery, *SIAM J. Numer. Anal.*, 42(4)(2004), 1780-1800.
- [17] V. V. Shaidurov and H. Xie, Richardson extrapolation for eigenvalue of discrete spectral problem on general mesh, *Comput. Technol.*, 12(3)(2007), 24-37.
- [18] L. B. Wahlbin, Superconvergence in Galerkin Finite Element Methods, *Lecture Notes in Mathematics*, Vol. 1605, Springer, Berlin, 1995.
- [19] J. Wang, A superconvergence analysis for finite element solutions by the least-squares surface fitting on irregular meshes for smooth problems, *J. Math. Study*, 33(3) (2000).
- [20] N.-E. Wiberg and X. D. Li, Superconvergence patch recovery of finite element solutions and a posteriori  $L_2$  norm error estimate, *Comm. Numer. Methods Engrg.*, 37 (1994), 313-320.
- [21] J. Xu and Z. Zhang, Analysis of recovery type a posteriori error estimators for mildly structured grids, *Math. Comp.*, 73 (2004), 1139-1152.
- [22] Z. Zhang, Ultraconvergence of the patch recovery technique II, *Math. Comp.*, 69 (2000), 141-158.
- [23] Z. Zhang, Polynomial preserving gradient recovery and a posteriori estimate for bilinear element on irregular quadrilaterals, *Int. J. Numer. Anal. Model.*, 1(2004), 1-24.
- [24] Z. Zhang and A. Naga, Validation of the a posteriori error estimator based on polynomial preserving recovery for linear elements, *Internat. J. Numer. Methods Engrg.*, 61 (2004), 1860-1893.
- [25] Z. Zhang and A. Naga, A new finite element gradient recovery method: Superconvergence property, *SIAM J. Sci. Comp.*, 26(4)(2005), 1192-1213.
- [26] Q. D. Zhu and Q. Lin, *Superconvergence Theory of the Finite Element Method*, Hunan Science Press, China, 1989 (in Chinese).
- [27] O. C. Zienkiewicz and J. Z. Zhu, The superconvergence patch recovery and a posteriori error estimates. Part 1: The recovery technique, *Internat. J. Numer. Methods Engrg.*, 33 (1992), 1331-1364.